A polydnavirus-encoded ANK protein has a negative impact on steroidogenesis and development

TITLE

A polydnavirus-encoded ANK protein has a negative impact on steroidogenesis and development

Authors and Affiliations

Marilena Ignesti [a], Rosalba Ferrara [b], Patrizia Romani [a, c], Luca Valzania [a, d], Giulia Serafini [a], Francesco Pennacchio [b, *], Valeria Cavaliere [a, **], Giuseppe Gargiulo [a, *]**

[a] Dipartimento di Farmacia e Biotecnologie, Università di Bologna, Via Selmi 3 Bologna, Italy.

[b] Dipartimento di Agraria – Laboratorio di Entomologia "E. Tremblay", Università di Napoli 'Federico II', Portici (NA), Italy.

[c] Present address: Dipartimento di Medicina Molecolare, Università di Padova, Padova, Italy.

[d] Present address: Department of Entomology, University of Georgia, Athens, GA 30602, USA.

[*] Corresponding author. Dipartimento di Agraria – Laboratorio di Entomologia "E. Tremblay", Università di Napoli 'Federico II', Portici (NA), Italy.

[**] Corresponding author. Dipartimento di Farmacia e Biotecnologie, Università di Bologna, Via Selmi 3 Bologna, Italy.

[***] Corresponding author. Dipartimento di Farmacia e Biotecnologie, Università di Bologna, Via Selmi 3 Bologna, Italy.

Abstract

Polydnaviruses (PDV) are viral symbionts associated with ichneumonid and braconid wasps parasitizing moth larvae, which are able to disrupt the host immune response and development, as well as a number of other physiological pathways. The immunosuppressive role of PDV has been more intensely investigated, while very little is known about the PDV-encoded factors disrupting host development. Here we address this research issue by further expanding the functional analysis of *ankyrin* genes encoded by the bracovirus associated with *Toxoneuron nigriceps* (Hymenoptera, Braconidae). In a previous study, using *Drosophila melanogaster* as experimental model system, we demonstrated the negative impact of *TnBVank1* impairing the ecdysone biosynthesis by altering endocytic traffic in prothoracic gland cells. With a similar approach here we demonstrate that another member of the viral *ank* gene family, *TnBVank3*, does also contribute to the disruption of ecdysone biosynthesis, but with a completely different mechanism. We show that its expression in *Drosophila* prothoracic gland (PG) blocks the larval-pupal transition by impairing the expression of steroidogenic genes. Furthermore, we found that *TnBVank3* affects the expression of genes involved in the insulin/TOR signaling and the constitutive activation of the insulin pathway in the PG rescues the pupariation impairment. Collectively, our data demonstrate that *Tn*BVANK3 acts as a virulence factor by exerting a synergistic and non-overlapping function with *Tn*BVANK1 to disrupt the ecdysone biosynthesis.

Keywords

Bracovirus; *Drosophila*; ANK proteins; Ecdysone biosynthesis; insulin/TOR signaling

1. Introduction

Parasitic wasps develop on a wealth of insect species, on which they induce a number of physiological and developmental alterations, which are essential to create a suitable environment for the development of their progeny (Pennacchio and Strand, 2006). These changes are currently denoted as host regulation, which is a complex process mediated by a network of molecular interactions, triggered and controlled by factors produced and released into the host by the ovipositing females (i.e. venom, microbial symbionts, ovarian secretions) and/or by the embryo (i.e. teratocytes, cells deriving from the dissociation of the embryonic membrane) or larvae (Pennacchio and Strand, 2006). Among microbial symbionts, polydnaviruses (PDVs) are potent immonosuppressive agents associated with ichneumonid and braconoid wasps parasitizing larval stages of moth larvae, and able to induce a number of pathological alterations in the host (Pennacchio and Strand, 2006; Strand and Burke, 2015). PDVs are integrated as proviruses in the wasp genome and replicate only in the epithelial cells of the ovarian calyx to produce free virions that are injected into the host at the oviposition. During this process they infect and express virulence factors in several host tissues, without undergoing replication (Herniou et al., 2013; Strand and Burke, 2015). The segmented genome of PDVs consists of multiple circles of DNA of different size, characterized by large non-coding segments and by genes showing an eukaryotic structure, often organized in gene families (Herniou et al., 2013; Strand and Burke, 2015). One of the most widespread gene family encodes ankyrin motif proteins (ANK), which are virtually expressed in all host tissues and found associated with a number of different pathological symptoms, ranging from immune to developmental alterations (Falabella et al., 2007; Strand and Burke, 2013). The viral ANK proteins have sequence similarity with members of IκB protein family, which

control the NF-κB signaling in insects and vertebrate innate immunity (Silverman and Maniatis, 2001). Due to the lack of the regulatory sequences needed for their signal-induced and basal degradation, these ANK proteins appear to irreversibly bind to host NF-κB factors and block their transcriptional activity. Therefore, a function as suppressors of the host immune system has been proposed and demonstrated for some members of PDV *ank* genes (Thoetkiattikul et al., 2005; Falabella et al., 2007; Bitra et al., 2012). In contrast, we know comparatively much less on the role of *ank* genes, and more in general of PDV-encoded factors, in the induction of host developmental alterations.

The host-parasitoid association *Heliothis virescens-Toxoneuron nigriceps* (Lepidoptera, Noctuidae - Hymenoptera, Braconidae) provides a valuable experimental model system to study the molecular bases of developmental arrest of mature larvae, which is due to a combined action of PDV and teratocytes, disrupting the biosynthetic activity of prothoracic glands (Pennacchio et al., 1997, 1998) and the ecdysteroid metabolism (Pennacchio et al., 1994a) respectively. Since the ecdysone biosynthesis is well conserved in insects (Niwa and Niwa, 2014), to identify whether *Tn*BV genes can disrupt this biosynthetic pathway, we took advantage of the *Drosophila melanogaster* model system that allow to design experiments that are not doable in *Heliothis*. The powerful molecular genetics techniques that can be applied in *Drosophila* (del Valle Rodriguez et al., 2011) allow the study of the effect that the expression of virulence genes has on specific tissues during development. Indeed, this model system has been even employed for studying human viral pathogens (Hughes et al., 2012).

Using this approach, in our previous work, we have gained insights on the role of a member of the viral *ank* gene family of *Tn*BV, *TnBVank1* (Duchi et al., 2010;

Valzania et al., 2014). We found that it functions as a virulence gene disrupting ecdysteroidogenesis in prothoracic gland by interfering with the endocytic trafficking of steroidogenic cells (Valzania et al., 2014). *Tn*BV genome carries two other members of the *ank* gene family (Falabella et al., 2007). In the present study we analyzed the effect of the expression of the *TnBVank3* in *Drosophila* steroidogenic cells. We found that also this gene contributes to the disruption of ecdysone biosynthesis by altering the expression of steroidogenic genes.

2. Materials and methods

2.1. Fly strains

Fly stocks were raised on standard cornmeal/yeast/agar medium at 18°C. *y* w^{67c23} was used as the wild type stock in this study. We used the following Bloomington stocks: #5138 (y^1 w^*; *P[tubP-Gal4]LL7/TM3,* Sb^1 Ser^1); #7019 (w^*; *P[*w^{+mC}*=tubP-*$Gal80^{ts}$*]20; TM2/TM6B,* Tb^1); #8263 y^1 w^{1118}; *P[UAS-InR.A1325D]2*. *phm-Gal4* (Ono et al., 2006) was a gift from C. Mirth (*phm-Gal4,UAS-mCD8::GFP/TM6B*).

2.2. Crosses

For the *tub-*$Gal80^{ts}$; *phm-Gal4* experiments, *tub-*$Gal80^{ts}$*; phm-Gal4/TM6B* females were crossed at 21°C to *UAS-TnBVank3* males, or to *y* w^{67c23} males as control. Larvae were raised at 21°C and transferred at 29°C at specific time points after egg laying (AEL). For the *UAS-*InR^{CA} *expression, tub-*$Gal80^{ts}$*; phm-Gal4/TM6B* females were crossed at 21°C to *UAS-*InR^{CA};*UAS-TnBVank3* males, and to *UAS-*InR^{CA} males as control. Larvae were raised at 21°C and transferred at 29°C after 3 days AEL.

2.3. Generation of TnBVank3-HA-Myc transgenic line

A construct containing the epitope tags hemagglutinin (*HA*) and *Myc* at the 3' end of of *TnBVank3* gene was produced (Biomatik) and cloned into the pUAST-attb vector (Bischof et al., 2007). The transgenic *Drosophila* line carrying the UAS-*TnBVank3-HA-Myc* chimeric gene was obtained by phiC31 integrase-mediated insertion into the attP2 landing-site locus on the third chromosome by BestGene Inc (USA).

2.4. Immunofluorescence microscopy

Immunostaining on ring glands was performed as described previously (Valzania et al., 2016). The *Tn*BVANK3-HA-Myc protein was detected using a polyclonal rabbit anti-HA 1:50 (Santa Cruz Biotechnology, USA) and anti-rabbit Cy3-conjugated 1:2000 (Invitrogen, USA). The glands were mounted in Fluoromount G (Electron Microscopy Sciences, USA) and analyzed with TCS SL Leica confocal system. Images were processed using Adobe Photoshop CS6.

2.5 Protein Extracts and Western Blot Analysis

UAS-TnBVank3-HA-Myc or control *y* w^{67c23} males were crossed at 25 °C to *tub-Gal4/TM3*. Third instar larvae were collected and the total protein extraction and blot analysis were performed as already described (Romani et al., 2016). The *Tn*BVANK3-HA-Myc protein was detected using a monoclonal mouse anti-HA 1:100 (Santa Cruz Biotechnology, USA) and ECL Plex anti-mouse Cy3 1:2500 (GE Healthcare, USA).

2.6. 20-E rescue experiments

Two groups of ten *tub-Gal80*^{ts}; *phm-Gal4/ UAS-TnBVank3* larvae, initially raised at 21°C for 3 days AEL and then transferred at 29°C for other 3 days were collected and

placed in new tubes with yeast paste supplemented with 20-hydroxyecdysone (Sigma) 1 mg/ml and kept at 29°C. As a control the same experiments were carried out on larvae of the same genotype fed with yeast paste containing an equal amount of ethanol.

2.7. Quantitative Real-Time PCR (qRT-PCR)

For *E74A*, *E75A* and steroidogenic gene expression experiments, total RNA was isolated from 3 independent biological samples of 5 larvae or prepupae. Total RNA was isolated using TRIzol reagent (Thermo Scientific), and DNA was removed by RNase-Free DNase Set (Ambion). qRT-PCR was performed on an ABI PRISM 7900 Real-Time PCR system (Applied Biosystems) by means of the Power SYBR-Green RNA-to-Ct-1-Step Kit (Applied Biosystems).

For the expression analysis of insulin and TOR pathway components, 15 brain-ring gland complexes (BRGCs) were dissected, in PBS buffer, from four independent biological samples. Total RNA was isolated using TRIzol reagent (Thermo Scientific), and contaminant DNA was removed by RNase-Free DNase Set (Ambion). cDNA synthesis was carried out with dT-primed M-MLV Reverse Transcriptase (LifeTechnologies). Quantitative PCR was carried out with FastStart SYBR Green Master Mix (Roche) on a QuantStudio 6 real-time thermal cycler.

The qRT-PCR primers used are listed in Table S1 in the supplementary material. For all of the genes examined, the reactions were conducted in technical triplicates. All transcript expression values were normalized to *Rpl23* gene.

2.8. Prothoracic gland size measurements

For measurements of the PG area, confocal images of PGs taken at 40X magnification were quantified with Photoshop CS6.

2.9. Statistical analysis

GraphPad Prism software was used for statistical analysis. Statistical significance was determined on the basis of unpaired *t*-test performed on the means and p values were calculated (*=$p<0.05$; **=$p<0.01$ and ***=$p<0.001$). $p<0.05$ was considered statistically significant. All results are expressed as the mean ± standard deviation (SD).

3. Results and Discussion

3.1. Expression of TnBVank3 in the prothoracic gland induces developmental arrest at third instar

*Tn*BVANK3 is 168 aa long and contains 3 ankyrin repeats (Fig. 1A). To test the effect of the viral *Tn*BVANK3 protein on *Drosophila* development we used the GAL4/UAS binary expression system (Brand and Perrimon, 1993). We produced *Drosophila* transgenic lines carrying a UAS transgene encoding *Tn*BVANK3 protein tagged at the C terminus with the hemagglutinin (HA) and c-Myc epitopes. The expression of the *TnBVank3-HA-Myc* gene (hereafter abbreviated as *TnBVank3*) was assessed using the ubiquitous *tubulin-Gal4* driver (*tub-Gal4*, hereafter abbreviated as *tub>*). The *Tn*BVANK3 protein was detected in third instar *tub>TnBVank3* larvae by western blot on whole cell lysate, using anti-HA antibody. A band in the size range of 23 kDa was detected, as expected for the *Tn*BVANK3-HA-Myc protein (Fig. 1B). No signal was observed in protein extracts from the control larvae *tub>+*. The ubiquitous expression of *TnBVank3* driven by the *tub>* driver did not affect larval development.

However, no *tub>TnBVank3* adult flies were obtained, since after pupariation the pupae degenerate (data not shown). This phenotype suggested that *TnBVank3* expression could affect metamorphosis, without any impact on larval molts, as observed in host larvae parasitized by *T. nigriceps* (Pennacchio et al., 1994b). Pulses of the hormone ecdysone (E) dictate the precise timing of the developmental transitions in *Drosophila*, such as larval molts, pupariation and metamorphosis (Warren et al., 2006). Ecdysone is synthesized in the steroidogenic cells of the prothoracic gland (PG) and secreted into the hemolymph, to reach peripheral tissues where it is converted to its active form, 20-hydroxyecdysone (20E). To test whether *Tn*BVANK3 affects *Drosophila* development impairing the prothoracic gland function, we specifically targeted the expression of *TnBVank3* in this gland using the *phantom-Gal4* driver (*phm-Gal4*, hereafter abbreviated as *phm>*), which allows high expression level of UAS transgene in the PG. We expressed *TnBVank3* in PG cells of larvae, at specific time points after egg laying (AEL) using a temperature sensitive form of the Gal4 repressor Gal80, $Gal80^{ts}$ (McGuire et al., 2003), which allows modulation of Gal4 activity. We used *tub-*$Gal80^{ts}$*; phm-Gal4* (**$Gal80^{ts}$*; phm>*) to control the timing of *TnBVank3* expression in the PG cells. **$Gal80^{ts}$*; phm>TnBVank3* and control **$Gal80^{ts}$*; phm>+* larvae were initially raised at 21°C, and at the early L2 stage (3 days AEL) were shifted to the restrictive temperature (29°C) to promote Gal4 activity. The temperature shift did not affect the normal development of control individuals. Conversely, at 29°C the larvae expressing *TnBVank3* exhibited a fully penetrant phenotype showing a block of larval-pupal transition, as observed in *H. virescens* larvae parasitized by *T. nigriceps* (Pennacchio et al., 1994b). After 2 days the **$Gal80^{ts}$*; phm>TnBVank3* larvae are similar in size to control larvae (Fig. 2A). However, at the third day, while control larvae pupate, **$Gal80^{ts}$*; phm>TnBVank3* do

not. During their prolonged L3 larval life that extended up to 3-4 weeks, the *Gal80^{ts}; phm>TnBVank3* larvae continue to increase in size (Fig. 2A). When the *Gal80^{ts}; phm>TnBVank3* larvae are shifted from 21°C to 29°C at 4 days AEL, some of them pupariated, while all the larvae shifted at 29°C, at 5 days AEL, regularly pupariated. Thus, when *TnBVank3* expression is triggered in the PG cells of L2 larvae it causes the block of pupariation.

3.2. TnBVank3 affects ecdysone activity

At the end of larval development a high peak of ecdysone triggers pupariation. In our experimental conditions (larvae initially raised at 21°C for 3 days AEL and then shifted to 29°C) in wild type larvae pupariation occurs after 3 days at 29°C with the formation of white prepupae. To investigate whether the block of the transition to pupal stage caused by the expression of *TnBVank3* was due to a low level of 20E, we carried out ecdysone-feeding rescue experiments. Third instar *Gal80^{ts}; phm>TnBVank3* larvae after 3 days at 29°C were transferred to new vials containing yeast paste supplemented with 20E dissolved in ethanol or just ethanol. After 24 h at 29°C all the larvae fed with 20E had developed into pupae (100%, n=20) (Fig. 2B). Conversely, the *Gal80^{ts}; phm>TnBVank3* larvae fed with yeast and ethanol, as a control, did not form any puparia and all of them persisted as third instar (n=20). This result indicates that the expression of *TnBVank3* in the PG impairs the biosynthesis of ecdysone. We therefore investigated the ecdysone activity by measuring the expression levels of two 20E-inducible transcription factors, *E74A* and *E75A*, which are required to undertake metamorphosis (Karim and Thummel, 1992) and can be used as readout for ecdysone levels. We induced *TnBVank3* expression in PG of larvae and, after 2 and 3 days at 29°C, we analyzed by qRT-PCR the expression levels

of *E74A* and *E75A* genes in *Gal80^{ts}; phm>TnBVank3* larvae and in *Gal80^{ts}; phm>+* control larvae/white prepupae of the same age (Fig. 2C). The expression of both *E74A* and *E75A* was significantly reduced in *TnBVank3* larvae (after 2 days at 29°C), as well as in larvae after 3 days at 29°C compared to the control white prepupae. Collectively these data indicate that in the *TnBVank3* larvae the ecdysone biosynthesis is impaired causing the block of larval development.

3.3. TnBVANK3 affects the expression of steroidogenic genes

Ecdysone is synthesized from cholesterol in the steroidogenic cells of the PG (Fig. 3A). Cholesterol, which cannot be synthesized by insects (Gilbert and Warren, 2005), enters the steroidogenic cells through a receptor-mediated low-density lipoprotein endocytic pathway (Rodenburg and Van der Horst, 2005), which delivers cholesterol to the endosomes. A number of ecdysone biosynthetic genes have been identified and characterized in *Drosophila* (Fig. 3A) (Gilbert and Warren, 2005; Niwa and Niwa, 2014). The first enzymatic reaction of the pathway, the conversion of cholesterol to 7-dehydrocholesterol (7dC) is catalyzed by Neverland (Nvd) (Yoshiyama et al., 2006; Yoshiyama-Yanagawa et al., 2011). 7dC is then converted to 5β-ketodiol (KD) through the 'Black Box', a biosynthetic step not yet characterized, in which Shroud (Sro), Spook (Spo) and Spookier (Spok) are involved (Namiki et al., 2005; Ono et al., 2006, 2012; Niwa et al., 2010). Phantom (Phm) transforms KD in ketotriol (KT), Disembodied (Dib) converts KT in 2-deoxyecdysone (2dE) and Shadow (Sad) converts 2dE to ecdysone (E) (Chavez et al., 2000; Warren et al., 2002, 2004; Petryk et al., 2003; Niwa et al., 2004). After release from the PG into the hemolymph, E is converted in peripheral tissues to its active form 20-hydroxyecdysone (20E) by Shade (Shd) enzyme (Petryk et al., 2003).

We investigated whether expression of steroidogenic genes was affected by *TnBVank3* expression in the PG cells. We compared by qRT-PCR the expression levels of *nvd*, *spok*, *sro*, *phm*, *dib* and *sad* genes in *Gal80^{ts}; phm>TnBVank3* larvae kept of 2 and 3 days at 29°C with that in *Gal80^{ts}; phm>+* control larvae kept of 2 days at 29°C and white prepupae of 3 days at 29°C (Fig. 3B). Expression of *TnBVank3* in the PG resulted in a down-regulation of steroidogenic genes, with a more pronounced effect on *nvd*, *spok* and *sro,* which catalyze early steps in the ecdysone biosynthetic pathway.

These data further support our finding that *Tn*BVANK3 impairs the ecdysone biosynthesis.

3.4. TnBVANK3 affects PG size

To investigate the *Tn*BVANK3 distribution in PG cells expressing the *TnBVank3* gene, we performed immunostaining experiments using an anti-HA antibody on *Gal80^{ts}; phm>TnBVank3* PGs of third instar larvae (after 2 days at 29°C). Interestingly, *Tn*BVANK3 was localized only in the nucleus of PG cells (Fig. 4A,B). Since, the *phm-Gal4* stock that we used carries the *UAS-mCD8::GFP* construct, the detection of the mCD8::GFP cell membrane marker allowed us to visualize the PGs (Fig. 4B). *TnBVank3* expression did not alter the gross morphology of the PG (compare Videos S1 and S2), although the PG size was smaller than in control PGs (-17.7% Fig. 4C), as observed also in parasitized tobacco budworm larvae (Pennacchio et al., 1997).

3.5. TnBVANK3 reduces the expression of the insulin/TOR signaling components

In *Drosophila*, as in the other holometabolous insects, metamorphosis can start after the larvae have reached the appropriate size, known as critical weight (CW). In *Drosophila* CW is attained in the early half of the L3 instar larvae. The achievement of CW is associated with the activation of steroidogenesis, which is controlled by a complex regulatory network of cross-modulating molecular events (Niwa and Niwa, 2016).

The prothoracicotropic hormone (PTTH) produced by the brain stimulates the synthesis of ecdysone by targeting its receptor Torso in the PG cells, which influences both the activation of ecdysone biosynthesis and CW control (McBrayer et al., 2007; Rewitz et al., 2009). The insulin/TOR (target of rapamycin) signaling, which controls growth rate and body size, do also promote growth of PG cells and their biosynthetic activity (timing and amount) (Yamanaka et al., 2013), is part of the complex molecular network assessing the CW and controlling the downstream developmental events (Koyama et al., 2014). It has been shown that increasing insulin signaling in the PG causes an increase of gland size and ecdysone biosynthesis, which results into a precocious metamorphosis, leading to pupae and adults of reduced size (Caldwell et al., 2005; Colombani et al., 2005; Mirth et al., 2005). Conversely, a down-regulation of the insulin signaling has a negative impact on gland size and ecdysone biosynthesis, which determines a delayed pupariation, giving rise to larger pupae and adults. A more severe phenotype is produced in response to the knock down of TOR, controlling the progression of PG endocycle required for activation of ecdysone biosynthesis, which determines a reduction of PG size and a down-regulation of ecdysteroidogenic genes associated with a developmental arrest of third instar larvae (Ohhara et al., 2017)

The negative effect of *TnBVank3* on the ecdysone biosynthesis and the PG size, coupled with a severe developmental arrest phenotype, produced when this gene is expressed from the L2 stage, before the CW is reached, suggested that *Tn*BVANK3 impairs the insulin/TOR signaling. To test this hypothesis, we investigated the mRNA levels of the insulin/TOR signaling components in the BRGCs of *Gal80^{ts}; phm>TnBVank3* and *Gal80^{ts} ; phm>+* control larvae kept for 2 days at 29°C. For the insulin pathway we found a significant reduced expression of *InR*, *Pi3K* and *Akt* genes (Fig. 5A). The analysis of the TOR pathway also revealed a significant decrease of the mRNA levels of *Tor* and the key downstream effector *S6 kinase* (*S6k*) (Fig. 5A).

We next investigated whether the activation of InR pathway could rescue the pupariation defect induced by *Tn*BVANK3. We found that the expression in the PG cells of a constitutively active form of the insulin receptor (InR^{CA}) was able to restore pupariation (Fig. 5B). Accordingly to the constitutive activation of insulin pathway, the control larva expressing only *InR^{CA}* advanced the onset of metamorphosis giving rise to small pupae (Caldwell et al., 2005; Colombani et al., 2005). This phenotype was also produced in the *InR^{CA}*; *TnBVank3* larvae.

Collectively, our data suggest that in the *TnBVank3* larvae the reduction of insulin/TOR signaling contributes to the negative effect on ecdysone biosynthesis. Although our findings indicate that a reduction of the expression of steroidogenic genes underlies the *Tn*BVANK3 developmental arrest phenotype, we cannot assert that this down-regulation is only due to the reduction of insulin/TOR signaling or whether *Tn*BVANK3 might also act directly on disrupting biosynthetic enzyme gene expression. However, if and how *Tn*BVANK3 may have an impact on other transduction pathways controlling steroidogenesis remains to be studied.

4. Conclusions

Our study on the viral *ank* gene *TnBVank3* clearly points out its role in blocking ecdysone biosynthesis. A similar effect was produced by the expression of another member of the same gene family, *TnBVank1* (Valzania et al., 2014). Interestingly, these two genes target different parts of the ecdysone biosynthetic pathway, while *Tn*BVANK3 localizes into the nucleus and causes a reduced expression of steroidogenic genes, *Tn*BVANK1 acts in the cytoplasm, by blocking the cholesterol trafficking. The high similarity of natural host phenotypes induced by the PDV infection with those we produced in the *Drosophila* model system, by expressing specific PDV genes, paves the way for further experiments on the natural host, aiming to shed light if the complementary and synergistic effects of these two virulence factors are adopted by parasitic wasps to ensure a complete block of host ecdysone biosynthesis and its larval development.

Figure captions

Fig. 1. Inducible expression of *Tn*BVANK3-HA-Myc chimeric protein. (A) Scheme showing the amino acid sequence of *Tn*BVANK3 and the HA and Myc epitopes fused at its carboxy terminus. The underlined Ankyrin repeat domains were predicted by searching the sequences using the SMART database (Simple Modular Architecture Research Tool; http://smart.embl-heidelberg.de/), using the default parameters (Schultz et al., 1998). (B) Western blot of third instar larvae cell lysate using anti-HA antibody. Larvae expressing the *UAS-TnBVank3-HA-Myc* transgene by the ubiquitous driver *tub-Gal4* show a band in the size range of 23 kDa that corresponds to the predicted *Tn*BVANK3-HA-Myc protein. This band is absent in control larvae *tub*>+ carrying only the Gal4 driver.

Fig. 2. *TnBVank3* expression in the PG cells affects the ecdysone biosynthesis causing the block of the transition from larval to pupal stage.
(A) Light micrographs of *Gal80^{ts}; phm>TnBVank3* and *Gal80^{ts}; phm>+* larvae of different ages at 29°C. (B) Rescue experiments of *Gal80^{ts}; phm>TnBVank3* with 20-hydroxyecdysone (20E). After 3 days at 29°C *Gal80^{ts}; phm>TnBVank3* larvae fed with medium supplemented with 20E induces the pupariation (red), while larvae fed with medium containing ethanol (EtOH) do not pupate (green). (C) qRT-PCR analyses of the mRNA levels of the 20E-inducible transcriptional factors (*E74A*, *E75A*) of *Gal80^{ts}; phm>+*and *Gal80^{ts}; phm>TnBVank3* of individuals kept at 29°C for the indicated days. Graphs represent mean ± SD; $n=3$; **=$p<0.01$; ***=$p<0.001$.

Fig. 3. *Tn*BVANK3 reduces the expression of genes of the ecdysone biosynthetic pathway. (A) Scheme showing the steps in the conversion of cholesterol to ecdysone (E). (B) qRT-PCR analysis of the transcript levels of the ecdysone biosynthetic enzymes of individuals of the reported genotypes kept at 29°C for the indicated days. Graphs represent mean ± SD; $n=3$; *=$p<0.05$; **=$p<0.01$; ***=$p<0.001$.

Fig. 4. *Tn*BVANK3 localization in the PG cells and its effects on PG size.
(A,B) Immunolocalization of *Tn*BVANK3-HA-Myc with anti-HA antibody (red) in PG cells of third instar *Gal80^{ts}; phm>TnBVank3* larvae (marked with mCD8::GFP, green, B). *Tn*BVANK3 shows a nuclear localization. (C) The *Gal80^{ts}; phm>TnBVank3* PGs are significantly smaller (-17.7%) than PGs from control *Gal80^{ts}; phm>+* larvae. The graph represents the mean ± SD; 16 *Gal80^{ts}; phm>TnBVank3* PGs and 10 *Gal80^{ts}; phm>+* PGs analyzed; **=$p<0.01$.

Fig. 5. *Tn*BVANK3 affects the expression of the insulin/TOR signaling components. (A) qRT-PCR analysis of the transcript levels of *InR, Pi3K, Akt, Tor* and *S6k* in the BRGC of the control and *TnBVank3* larvae that were raised at 21°C for 3 days AEL and then kept at 29°C for 2 days. Graphs represent mean ± SD; $n=4$; *=$p<0.05$; **=$p<0.01$; ***=$p<0.001$. (B) Coexpression in the PGs of *TnBVank3* and the constitutively active form of insulin receptor (InR^{CA}). Activation of insulin signaling restores pupariation in *TnBVank3* larvae. The described results were obtained by analyzing larvae raised at 21°C for 3 days AEL and then were shifted to the 29°C restrictive temperature.

Video captions

Video S1

Morphology of a PG gland expressing *TnBVank3* and the cell membrane marker mCD8::GFP.

QuickTime movie of 50 confocal optical z stack sections each with a scan step size of 0.33 µm through the entire PG. The detection of the mCD8::GFP protein allow to visualize the PG morphology.

Video S2

Morphology of a PG gland expressing the cell membrane marker mCD8::GFP.

QuickTime movie of 41 confocal optical z stack sections each with a scan step size of 0.33 µm through the entire PG. The detection of the mCD8::GFP protein allow to visualize the PG morphology.

Acknowledgements

We thank Christen Mirth and Bloomington Stock Center for fly stocks. We thank Davide Andrenacci for helpful suggestions and critical reading of the manuscript. The work was supported by a research grant from University of Bologna (RFO 2014) to GG and VC; by the project POR Campania FESR 2007-2013 Bio Industrial Processes-BIP, and the project Safe & Smart (Cluster Agroalimentare Nazionale - CTN01_00230_248064) to FP.

Authors' contribution

VC, GG and FP conceived the research. MI, PR, LV and GS performed *Drosophila* experimental work and morphological analyses. RF and PR performed qRT-PCR analyses. MI conceived and designed part of the experiments. VC, FP and GG wrote the manuscript.

REFERENCES

Bischof, J., Maeda, R.K., Hediger, M., Karch, F., Basler, K., 2007. An optimized transgenesis system for Drosophila using germ-line-specific phiC31 integrases. Proc Natl Acad Sci U S A 104, 3312-3317.

Bitra, K., Suderman, R.J., Strand, M.R., 2012. Polydnavirus Ank proteins bind NF-kappaB homodimers and inhibit processing of Relish. PLoS Pathog 8, e1002722.

Brand, A.H., Perrimon, N., 1993. Targeted gene expression as a means of altering cell fates and generating dominant phenotypes. Development 118, 401-415.

Caldwell, P.E., Walkiewicz, M., Stern, M., 2005. Ras activity in the Drosophila prothoracic gland regulates body size and developmental rate via ecdysone release. Curr Biol 15, 1785-1795.

Chavez, V.M., Marques, G., Delbecque, J.P., Kobayashi, K., Hollingsworth, M., Burr, J., Natzle, J.E., O'Connor, M.B., 2000. The Drosophila disembodied gene controls late embryonic morphogenesis and codes for a cytochrome P450 enzyme that regulates embryonic ecdysone levels. Development 127, 4115-4126.

Colombani, J., Bianchini, L., Layalle, S., Pondeville, E., Dauphin-Villemant, C., Antoniewski, C., Carre, C., Noselli, S., Leopold, P., 2005. Antagonistic actions of ecdysone and insulins determine final size in Drosophila. Science 310, 667-670.

del Valle Rodriguez, A., Didiano, D., Desplan, C., 2011. Power tools for gene expression and clonal analysis in Drosophila. Nat Methods 9, 47-55.

Duchi, S., Cavaliere, V., Fagnocchi, L., Grimaldi, M.R., Falabella, P., Graziani, F., Gigliotti, S., Pennacchio, F., Gargiulo, G., 2010. The impact on microtubule network of a bracovirus IkappaB-like protein. Cell Mol Life Sci 67, 1699-1712.
Falabella, P., Varricchio, P., Provost, B., Espagne, E., Ferrarese, R., Grimaldi, A., de Eguileor, M., Fimiani, G., Ursini, M.V., Malva, C., Drezen, J.M., Pennacchio, F., 2007. Characterization of the IkappaB-like gene family in polydnaviruses associated with wasps belonging to different Braconid subfamilies. J Gen Virol 88, 92-104.
Gilbert, L.I., Warren, J.T., 2005. A molecular genetic approach to the biosynthesis of the insect steroid molting hormone. Vitam Horm 73, 31-57.
Herniou, E.A., Huguet, E., Theze, J., Bezier, A., Periquet, G., Drezen, J.M., 2013. When parasitic wasps hijacked viruses: genomic and functional evolution of polydnaviruses. Philos Trans R Soc Lond B Biol Sci 368, 20130051.
Hughes, T.T., Allen, A.L., Bardin, J.E., Christian, M.N., Daimon, K., Dozier, K.D., Hansen, C.L., Holcomb, L.M., Ahlander, J., 2012. Drosophila as a genetic model for studying pathogenic human viruses. Virology 423, 1-5.
Karim, F.D., Thummel, C.S., 1992. Temporal coordination of regulatory gene expression by the steroid hormone ecdysone. EMBO J 11, 4083-4093.
Koyama, T., Rodrigues, M.A., Athanasiadis, A., Shingleton, A.W., Mirth, C.K., 2014. Nutritional control of body size through FoxO-Ultraspiracle mediated ecdysone biosynthesis. Elife 3.
McBrayer, Z., Ono, H., Shimell, M., Parvy, J.P., Beckstead, R.B., Warren, J.T., Thummel, C.S., Dauphin-Villemant, C., Gilbert, L.I., O'Connor, M.B., 2007. Prothoracicotropic hormone regulates developmental timing and body size in Drosophila. Dev Cell 13, 857-871.
McGuire, S.E., Le, P.T., Osborn, A.J., Matsumoto, K., Davis, R.L., 2003. Spatiotemporal rescue of memory dysfunction in Drosophila. Science 302, 1765-1768.
Mirth, C., Truman, J.W., Riddiford, L.M., 2005. The role of the prothoracic gland in determining critical weight for metamorphosis in Drosophila melanogaster. Curr Biol 15, 1796-1807.
Namiki, T., Niwa, R., Sakudoh, T., Shirai, K., Takeuchi, H., Kataoka, H., 2005. Cytochrome P450 CYP307A1/Spook: a regulator for ecdysone synthesis in insects. Biochem Biophys Res Commun 337, 367-374.
Niwa, R., Matsuda, T., Yoshiyama, T., Namiki, T., Mita, K., Fujimoto, Y., Kataoka, H., 2004. CYP306A1, a cytochrome P450 enzyme, is essential for ecdysteroid biosynthesis in the prothoracic glands of Bombyx and Drosophila. J Biol Chem 279, 35942-35949.
Niwa, R., Namiki, T., Ito, K., Shimada-Niwa, Y., Kiuchi, M., Kawaoka, S., Kayukawa, T., Banno, Y., Fujimoto, Y., Shigenobu, S., Kobayashi, S., Shimada, T., Katsuma, S., Shinoda, T., 2010. Non-molting glossy/shroud encodes a short-chain dehydrogenase/reductase that functions in the 'Black Box' of the ecdysteroid biosynthesis pathway. Development 137, 1991-1999.
Niwa, R., Niwa, Y.S., 2014. Enzymes for ecdysteroid biosynthesis: their biological functions in insects and beyond. Biosci Biotechnol Biochem 78, 1283-1292.
Niwa, Y.S., Niwa, R., 2016. Transcriptional regulation of insect steroid hormone biosynthesis and its role in controlling timing of molting and metamorphosis. Dev Growth Differ 58, 94-105.
Ohhara, Y., Kobayashi, S., Yamanaka, N., 2017. Nutrient-Dependent Endocycling in Steroidogenic Tissue Dictates Timing of Metamorphosis in Drosophila melanogaster. PLoS Genet 13, e1006583.

456 Ono, H., Morita, S., Asakura, I., Nishida, R., 2012. Conversion of 3-oxo steroids into
457 ecdysteroids triggers molting and expression of 20E-inducible genes in Drosophila
458 melanogaster. Biochem Biophys Res Commun 421, 561-566.
459 Ono, H., Rewitz, K.F., Shinoda, T., Itoyama, K., Petryk, A., Rybczynski, R., Jarcho,
460 M., Warren, J.T., Marques, G., Shimell, M.J., Gilbert, L.I., O'Connor, M.B., 2006.
461 Spook and Spookier code for stage-specific components of the ecdysone biosynthetic
462 pathway in Diptera. Dev Biol 298, 555-570.
463 Pennacchio, F., Bradleigh Vinson, S., Tremblay, E., Ostuni, A., 1994a. Alteration of
464 ecdysone metabolism in Heliothis virescens (F.) (Lepidoptera: Noctuidae) larvae
465 induced by Cardiochiles nigriceps Viereck (Hymenoptera: Braconidae) teratocytes.
466 Insect Biochemistry and Molecular Biology 24, 383-394.
467 Pennacchio, F., Falabella, P., Sordetti, R., Paola, V., Malva, C., Bradleigh Vinson, S.,
468 1998. Prothoracic gland inactivation in Heliothis virescens (F.)
469 (Lepidoptera:Noctuidae) larvae parasitized by Cardiochiles nigriceps Viereck
470 (Hymenoptera:Braconidae). Journal of Insect Physiology 44, 845-857.
471 Pennacchio, F., Sordetti, R., Falabella, P., Vinson, S.B., 1997. Biochemical and
472 ultrastructural alterations in prothoracic glands of Heliothis virescens (F.)
473 (Lepidoptera: Noctuidae) last instar larvae parasitized by Cardiochiles nigriceps
474 Viereck (Hymenoptera: Braconidae). Insect Biochemistry and Molecular Biology 27,
475 439-450.
476 Pennacchio, F., Strand, M.R., 2006. Evolution of developmental strategies in parasitic
477 hymenoptera. Annu Rev Entomol 51, 233-258.
478 Pennacchio, F., Vinson, S.B., Tremblay, E., Tanaka, T., 1994b. Biochemical and
479 developmental alterations of Heliothis virescens (F.) (lepidoptera, noctuidae) larvae
480 induced by the endophagous parasitoid Cardiochiles nigriceps viereck (Hymenoptera,
481 braconidae). Archives of Insect Biochemistry and Physiology 26, 211-233.
482 Petryk, A., Warren, J.T., Marques, G., Jarcho, M.P., Gilbert, L.I., Kahler, J., Parvy,
483 J.P., Li, Y., Dauphin-Villemant, C., O'Connor, M.B., 2003. Shade is the Drosophila
484 P450 enzyme that mediates the hydroxylation of ecdysone to the steroid insect
485 molting hormone 20-hydroxyecdysone. Proc Natl Acad Sci U S A 100, 13773-13778.
486 Rewitz, K.F., Yamanaka, N., Gilbert, L.I., O'Connor, M.B., 2009. The insect
487 neuropeptide PTTH activates receptor tyrosine kinase torso to initiate metamorphosis.
488 Science 326, 1403-1405.
489 Rodenburg, K.W., Van der Horst, D.J., 2005. Lipoprotein-mediated lipid transport in
490 insects: analogy to the mammalian lipid carrier system and novel concepts for the
491 functioning of LDL receptor family members. Biochim Biophys Acta 1736, 10-29.
492 Romani, P., Papi, A., Ignesti, M., Soccolini, G., Hsu, T., Gargiulo, G., Spisni, E.,
493 Cavaliere, V., 2016. Dynamin controls extracellular level of Awd/Nme1 metastasis
494 suppressor protein. Naunyn Schmiedebergs Arch Pharmacol 389, 1171-1182.
495 Schultz, J., Milpetz, F., Bork, P., Ponting, C.P., 1998. SMART, a simple modular
496 architecture research tool: identification of signaling domains. Proc Natl Acad Sci U S
497 A 95, 5857-5864.
498 Silverman, N., Maniatis, T., 2001. NF-kappaB signaling pathways in mammalian and
499 insect innate immunity. Genes Dev 15, 2321-2342.
500 Strand, M.R., Burke, G.R., 2013. Polydnavirus-wasp associations: evolution, genome
501 organization, and function. Curr Opin Virol 3, 587-594.
502 Strand, M.R., Burke, G.R., 2015. Polydnaviruses: From discovery to current insights.
503 Virology 479-480, 393-402.

504 Thoetkiattikul, H., Beck, M.H., Strand, M.R., 2005. Inhibitor kappaB-like proteins
505 from a polydnavirus inhibit NF-kappaB activation and suppress the insect immune
506 response. Proc Natl Acad Sci U S A 102, 11426-11431.
507 Valzania, L., Ono, H., Ignesti, M., Cavaliere, V., Bernardi, F., Gamberi, C., Lasko, P.,
508 Gargiulo, G., 2016. Drosophila 4EHP is essential for the larval-pupal transition and
509 required in the prothoracic gland for ecdysone biosynthesis. Dev Biol 410, 14-23.
510 Valzania, L., Romani, P., Tian, L., Li, S., Cavaliere, V., Pennacchio, F., Gargiulo, G.,
511 2014. A polydnavirus ANK protein acts as virulence factor by disrupting the function
512 of prothoracic gland steroidogenic cells. PLoS One 9, e95104.
513 Warren, J.T., Petryk, A., Marques, G., Jarcho, M., Parvy, J.P., Dauphin-Villemant, C.,
514 O'Connor, M.B., Gilbert, L.I., 2002. Molecular and biochemical characterization of
515 two P450 enzymes in the ecdysteroidogenic pathway of Drosophila melanogaster.
516 Proc Natl Acad Sci U S A 99, 11043-11048.
517 Warren, J.T., Petryk, A., Marques, G., Parvy, J.P., Shinoda, T., Itoyama, K.,
518 Kobayashi, J., Jarcho, M., Li, Y., O'Connor, M.B., Dauphin-Villemant, C., Gilbert,
519 L.I., 2004. Phantom encodes the 25-hydroxylase of Drosophila melanogaster and
520 Bombyx mori: a P450 enzyme critical in ecdysone biosynthesis. Insect Biochem Mol
521 Biol 34, 991-1010.
522 Warren, J.T., Yerushalmi, Y., Shimell, M.J., O'Connor, M.B., Restifo, L.L., Gilbert,
523 L.I., 2006. Discrete pulses of molting hormone, 20-hydroxyecdysone, during late
524 larval development of Drosophila melanogaster: correlations with changes in gene
525 activity. Dev Dyn 235, 315-326.
526 Yamanaka, N., Rewitz, K.F., O'Connor, M.B., 2013. Ecdysone control of
527 developmental transitions: lessons from Drosophila research. Annu Rev Entomol 58,
528 497-516.
529 Yoshiyama, T., Namiki, T., Mita, K., Kataoka, H., Niwa, R., 2006. Neverland is an
530 evolutionally conserved Rieske-domain protein that is essential for ecdysone
531 synthesis and insect growth. Development 133, 2565-2574.
532 Yoshiyama-Yanagawa, T., Enya, S., Shimada-Niwa, Y., Yaguchi, S., Haramoto, Y.,
533 Matsuya, T., Shiomi, K., Sasakura, Y., Takahashi, S., Asashima, M., Kataoka, H.,
534 Niwa, R., 2011. The conserved Rieske oxygenase DAF-36/Neverland is a novel
535 cholesterol-metabolizing enzyme. J Biol Chem 286, 25756-25762.

Table S1. The primers used for qRT-PCR experiments

Gene	Forward	Reverse
nvd	5’-ACCTCCCCCTTATCCAAATG-3’	5’-AGCAACGCTTCCACCAATAC-3’
sro	5’-ATGAGCGGCAGTCAACTTCT-3’	5’-CAGGAAATCACGGTCATGTG-3’
spok	5’-TATCTCTTGGGCACACTCGCTG-3’	5’-GCCGAGCTAAATTTCTCCGCTT-3’
phm	5’-TCGTCGTGGGCGATTATTTTA-3’	5’-AAGGCCACTGGGTCCATGT-3’
dib	5’-TGCCCTCAATCCCTATCTGGTC-3’	5’-ACAGGGTCTTCACACCCATCTC-3’
sad	5’-AAGGAGCGAGCTACCAATGA-3’	5’-GCTGCTCAAAGTGTGATGGA-3’
E74A	5’-GCCCTTTATCGACGATGCAC-3’	5’-GCTCCATTCAGTTCGTTGCC-3’
E75A	5’-ACGGATATCAGCAGGCCAATC-3’	5’-GAATGCACGCCGTAATGGAAAC-3’
Rpl23	5’-GCTCAGGAAGAAGGTCATGC-3’	5’-GGCTATAGAGCTTGCATTGGA-3’
Akt	5’-GCCAGATCATGACCGTCGAT-3’	5’-GTCATAGCCACCTCACCCAC-3’
InR	5’-TTCTCTGGGAAATGGCCACC-3’	5’-TCGCCGAAGACCTATGATGC-3’
Pi3K	5’-GCCAGAACTGTCCTCCGAAA-3’	5’-CTTCGCTGAATTTCGCTCGG-3’
Tor	5’-GCTATGACGAGGCGAATGGA-3’	5’-TCTTGGGGAACAGCGTCTTC-3’
S6k	5’-GCCAGGAGACCATACAGCTC-3’	5’-TGCCATAACCACCTTTGCCA-3’

Figure 1

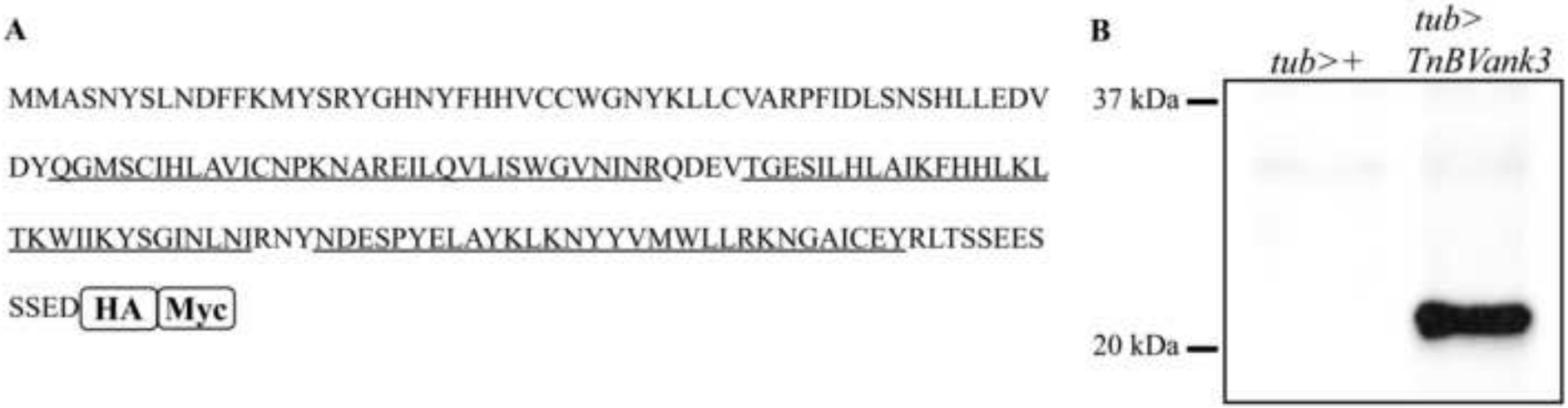
A
MMASNYSLNDFFKMYSRYGHNYFHHVCCWGNYKLLCVARPFIDLSNSHLLEDV
DYQGMSCIHLAVICNPKNAREILQVLISWGVNINRQDEVTGESILHLAIKFHHLKL
TKWIIKYSGINLNIRNYNDESPYELAYKLKNYYVMWLLRKNGAICEYRLTSSEES
SSED HA Myc
B
tub>+
tub> TnBVank3
37 kDa
20 kDa

Figure 2

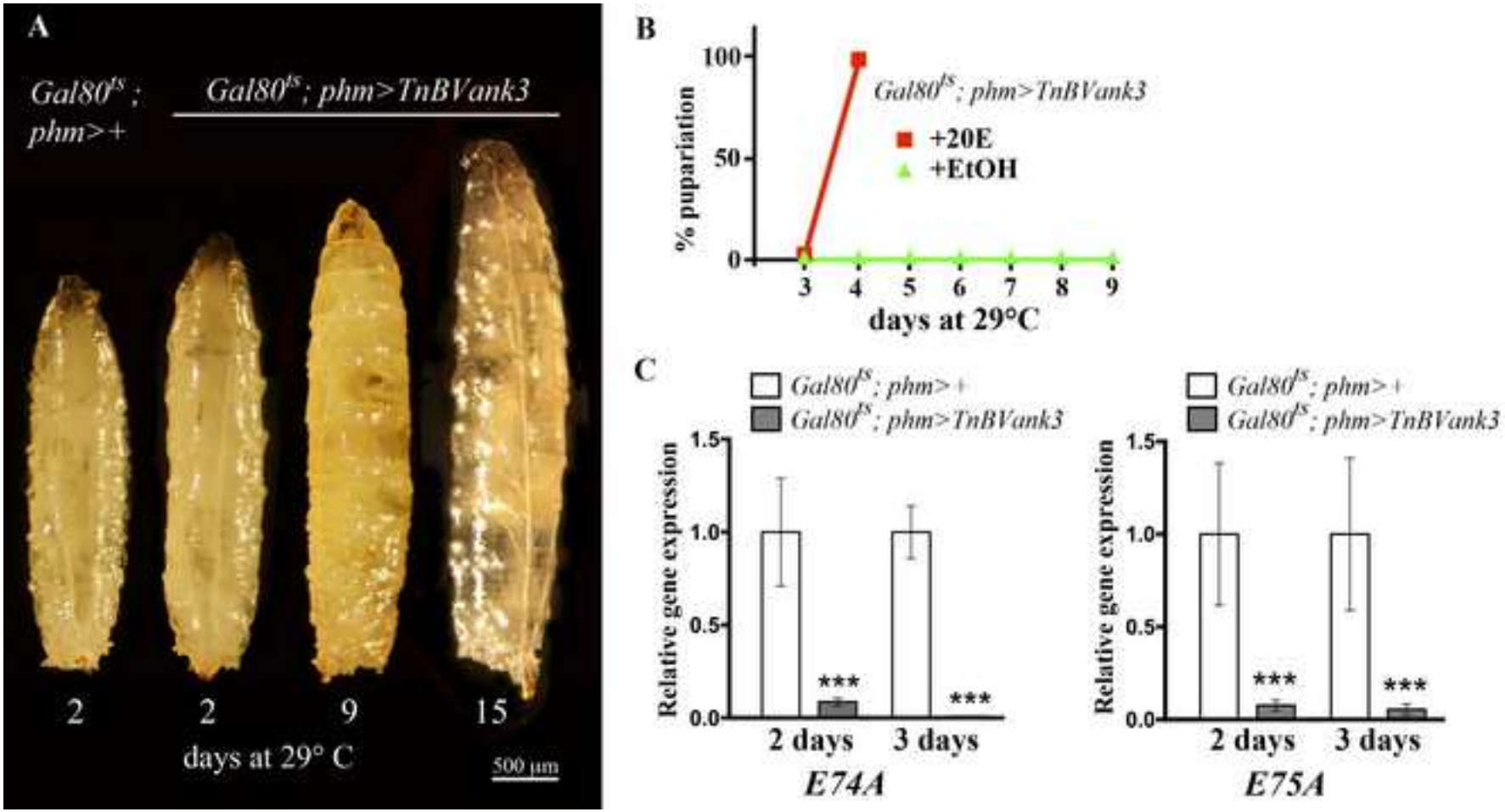
A
Gal80ts ; phm>+
Gal80ts ; phm>TnBVank3
2
2
9
15
days at 29° C
500 µm
B
% pupariation
100
50
0
Gal80ts ; phm>TnBVank3
+20E
+EtOH
3
4
5
6
7
8
9
days at 29°C
C
Gal80ts ; phm>+
Gal80ts ; phm>TnBVank3
Relative gene expression
1.5
1.0
0.5
0.0
***
***
2 days
3 days
E74A
Gal80ts ; phm>+
Gal80ts ; phm>TnBVank3
Relative gene expression
1.5
1.0
0.5
0.0
***
***
2 days
3 days
E75A

Figure 3

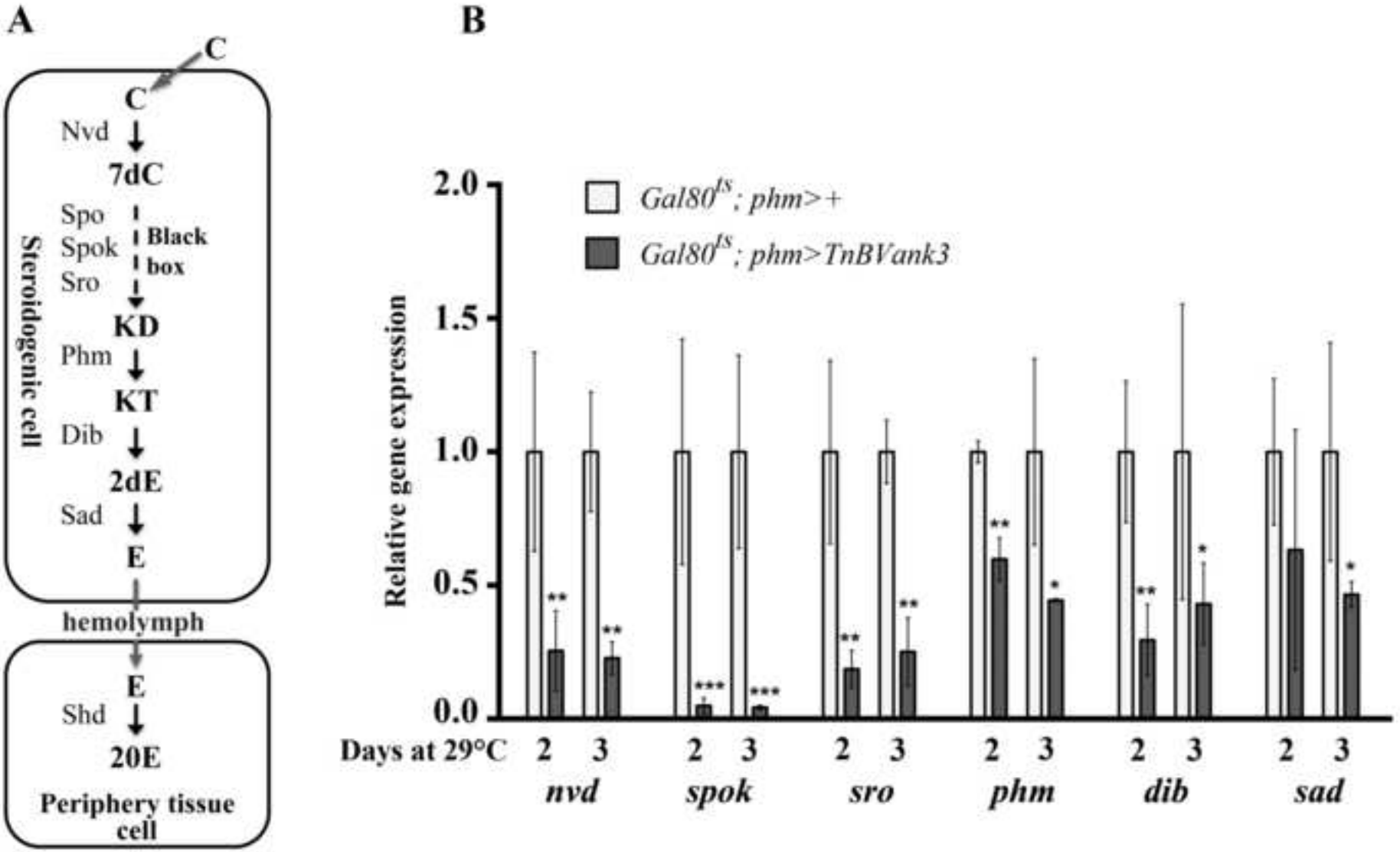
A
C
C
Nvd
7dC
Spo
Spok
Sro
Black box
KD
Phm
KT
Dib
2dE
Sad
E
Steroidogenic cell
hemolymph
E
Shd
20E
Periphery tissue cell
B
Gal80ts; phm>+
Gal80ts; phm>TnBVank3
Relative gene expression
2.0
1.5
1.0
0.5
0.0
Days at 29°C
2 3 2 3 2 3 2 3 2 3 2 3
nvd
spok
sro
phm
dib
sad

Figure 4

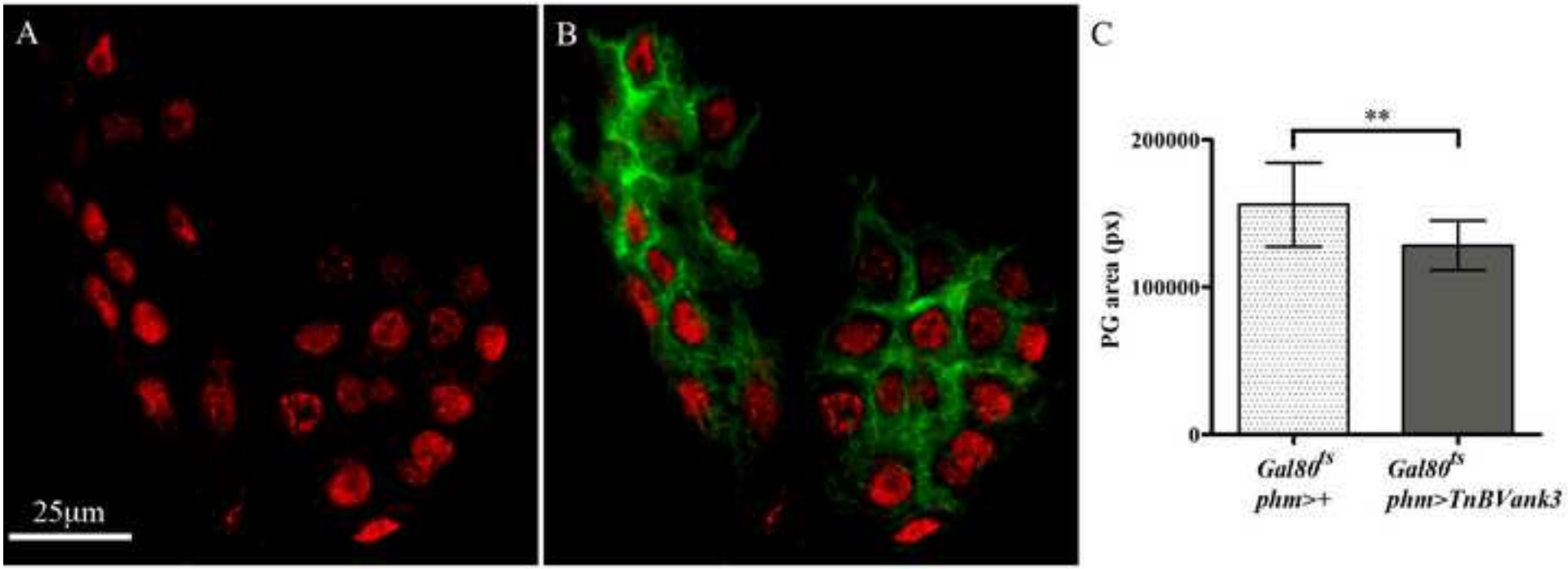
A
25μm
B
C
**
200000
100000
0
PG area (px)
Gal80ts
phm>+
Gal80ts
phm>TnBVank3

Figure 5

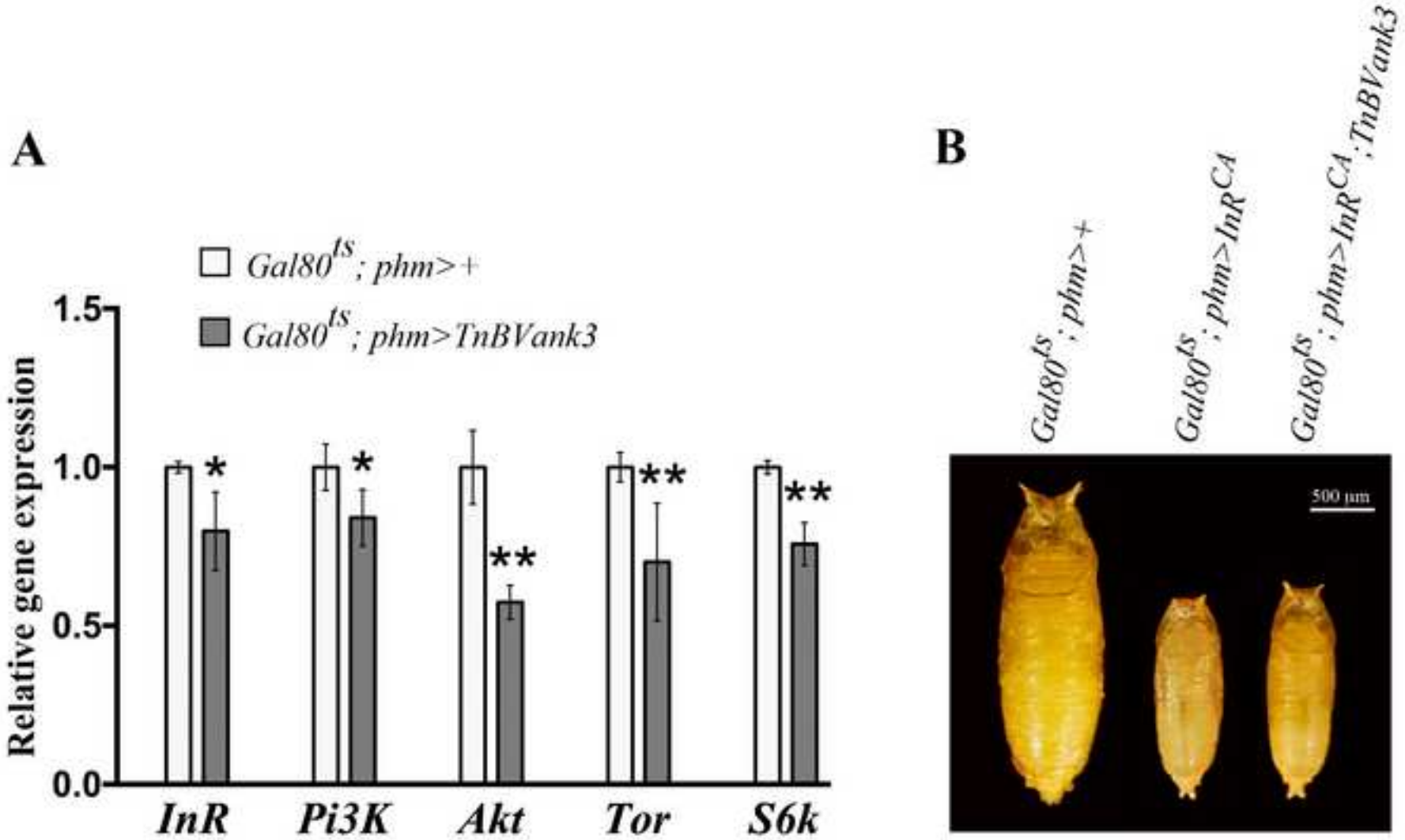
A
Gal80ts; phm>+
Gal80ts; phm>TnBVank3
Relative gene expression
1.5
1.0
0.5
0.0
*
*
**
**
**
InR
Pi3K
Akt
Tor
S6k
B
Gal80ts; phm>+
Gal80ts; phm>InRCA
Gal80ts; phm>InRCA; TnBVank3
500 μm